

An Implementation-Oriented Iris Recognition Algorithm Using Phase-Based Image Matching

Kazuyuki Miyazawa*, Koichi Ito*, Takafumi Aoki*, Koji Kobayashi† and Hiroshi Nakajima†

*Graduate School of Information Sciences, Tohoku University
Sendai 980-8579 Japan

Tel: +81-22-795-7169, Fax: +81-22-263-9308

E-mail: miyazawa@aoki.ecei.tohoku.ac.jp

†Yamatake Corporation, Tokyo, 140-0002, Japan

Tel: +81-3-6810-1324, E-mail: kobayashi-koji@jp.yamatake.com

Abstract—This paper presents a phase-based iris recognition algorithm which is specially designed for system implementation. In order to reduce the size of registration iris data and to prevent the visibility of iris images, we introduce the idea of 2D Fourier Phase Code (2D FPC) for representing iris information. 2D FPC corresponds to the quantized version of phase-spectrum of an iris image, which is essential for phase-based iris recognition. By the use of 2D FPC, while keeping a sufficient level of performance, the size of iris data can be reduced to below one-quarter compared to using iris image directly as the registration data. 2D FPC is particularly useful for implementing compact iris recognition devices using state-of-the-art DSP (Digital Signal Processing) technology.

I. INTRODUCTION

Biometric authentication has been receiving extensive attention over the past decade with increasing demands in automated personal identification [1]. Among many biometric techniques, iris recognition has gained much attention due to its high reliability for personal identification [2], [3], [4].

A major approach for iris recognition today is to generate feature vectors from individual iris images and to perform iris matching based on some distance metrics [2], [4]. Most of the commercial iris recognition systems implement a famous algorithm using *iris codes* proposed by Daugman [2]. One of the difficult problems in feature-based iris recognition is that the matching performance is significantly influenced by many parameters in feature extraction process (e.g., spatial position, orientation, center frequencies and size parameters for 2D Gabor filter kernel), which may vary depending on environmental factors of iris image acquisition.

Addressing the problem, we have proposed an efficient iris recognition algorithm [5], [6] using phase-based image matching — an image matching technique using phase components in 2D Discrete Fourier Transforms (DFTs) of given images. The proposed algorithm achieves very low error rate (EER=0.0032%) for CASIA iris image database [7]. In this paper, we discuss modification of the proposed algorithm dedicated to system implementation.

The proposed algorithm assumes the use of iris images directly in the system to achieve high recognition performance. But from the viewpoint of system implementation, this might bring about the increase of the registered data size and

undesirable visibility of iris image. In order to reduce the size of iris data and to prevent the visibility of individual iris images, we introduce 2D Fourier Phase Code (2D FPC) for representing iris information. 2D FPC is particularly useful for implementing compact iris recognition devices using state-of-the-art DSP (Digital Signal Processing) technology. By changing the degree of quantization in 2D FPC, we can optimize the trade-off between iris data size and recognition performance flexibly, while avoiding visibility of individual iris images.

II. IMPLEMENTATION-ORIENTED IRIS RECOGNITION ALGORITHM

This section describes the modification of the proposed iris recognition algorithm dedicated to system implementation. Fig. 1(a) shows the original algorithm for iris recognition, which consists of a preprocessing stage and a matching stage. We briefly overview these stages.

A. Preprocessing

An iris image contains some irrelevant parts (e.g., eyelid, sclera, pupil, etc.). Also, the size of an iris may vary depending on camera-to-eye distance and lighting condition. Therefore, the original image needs to be normalized.

(i) **Iris Localization:** This step is to detect the inner (iris/pupil) boundary and the outer (iris/sclera) boundary in the original image. We model the inner boundary as an ellipse, and the outer boundary as a circle.

(ii) **Iris Normalization:** Next step is to normalize iris images to compensate for iris deformation. In order to avoid eyelashes, we use only lower half portion of the iris (Fig. 1(b)) and unwrap the region to a rectangular block of a fixed size (256×128 pixels) as illustrated in Fig. 1(c). The eyelid region is then masked as in Fig. 1(d).

B. Matching

The key idea of the proposed algorithm is to use phase-based image matching for image alignment and matching score calculation (see Fig. 1(a)). Before discussing the algorithm, we introduce the principle of phase-based image matching using the Phase-Only Correlation (POC) function.

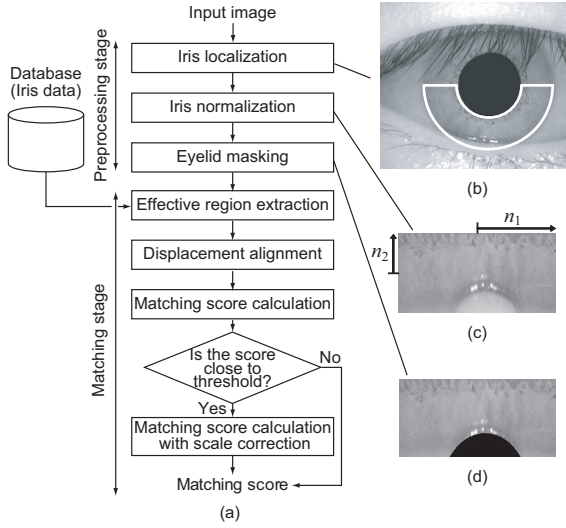


Fig. 1. Original algorithm: (a) flow diagram, (b) original image, (c) normalized image (n_1 axis corresponds to the angle of polar coordinate system and n_2 axis corresponds to the radius), and (d) normalized image with eyelid masking.

Consider two $N_1 \times N_2$ -pixel images, $f(n_1, n_2)$ and $g(n_1, n_2)$, where we assume that the index ranges are $n_1 = -M_1, \dots, M_1$ ($M_1 > 0$) and $n_2 = -M_2, \dots, M_2$ ($M_2 > 0$) for mathematical simplicity, and hence $N_1 = 2M_1 + 1$ and $N_2 = 2M_2 + 1$. Let $F(k_1, k_2)$ and $G(k_1, k_2)$ denote the 2D DFTs of the two images. The cross-phase spectrum $R_{FG}(k_1, k_2)$ is given by

$$R_{FG}(k_1, k_2) = \frac{F(k_1, k_2)\overline{G(k_1, k_2)}}{|F(k_1, k_2)G(k_1, k_2)|} = e^{j\theta(k_1, k_2)}, \quad (1)$$

where $k_1 = -M_1, \dots, M_1$, $k_2 = -M_2, \dots, M_2$, $\overline{G(k_1, k_2)}$ is the complex conjugate of $G(k_1, k_2)$ and $\theta(k_1, k_2)$ denotes the phase difference of $F(k_1, k_2)$ and $G(k_1, k_2)$. The POC function $r_{fg}(n_1, n_2)$ is the 2D Inverse DFT (IDFT) of $R_{FG}(k_1, k_2)$.

When two images are similar, their POC function gives a distinct sharp peak. When they are not similar, the peak drops significantly. The height of the peak gives a good similarity measure for image matching, and the location of the peak shows the translational displacement between the images.

Our observation shows that the 2D DFT of a normalized iris image contains meaningless phase components in high frequency domain, and that the effective frequency band of the normalized iris image is wider in k_1 direction than in k_2 direction (see Fig. 2). To evaluate the similarity using the inherent frequency band within iris textures, we employ BLPOC (Band-Limited Phase-Only Correlation) function.

Assume that the ranges of the significant frequency band are $k_1 = -K_1, \dots, K_1$ ($0 \leq K_1 \leq M_1$) and $k_2 = -K_2, \dots, K_2$ ($0 \leq K_2 \leq M_2$), where as shown in Fig. 2(b). Thus, the effective size of frequency spectrum is given by $L_1 = 2K_1 + 1$ and

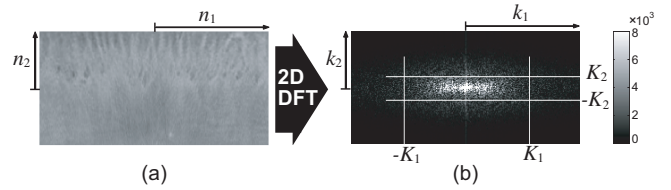


Fig. 2. Normalized iris image in (a) spatial domain, and in (b) frequency domain (amplitude spectrum), where $K_1 = 0.55M_1$ and $K_2 = 0.2M_2$.

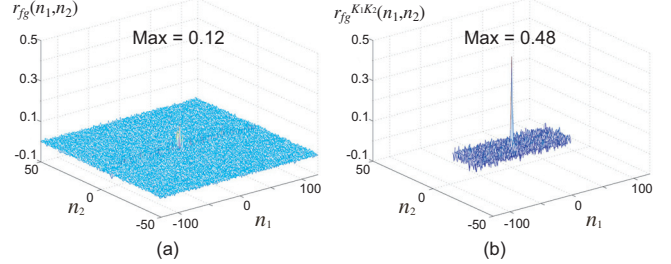


Fig. 3. Example of genuine matching using the original POC function and the BLPOC function: (a) original POC function $r_{fg}(n_1, n_2)$, and (b) BLPOC function $r_{fg}^{K_1 K_2}(n_1, n_2)$.

$L_2 = 2K_2 + 1$. The BLPOC function is given by

$$r_{fg}^{K_1 K_2}(n_1, n_2) = \frac{1}{L_1 L_2} \sum_{k_1, k_2} R_{FG}(k_1, k_2) W_{L_1}^{-k_1 n_1} W_{L_2}^{-k_2 n_2}, \quad (2)$$

where $n_1 = -K_1, \dots, K_1$, $n_2 = -K_2, \dots, K_2$, $W_{L_1} = e^{-j\frac{2\pi}{L_1}}$, $W_{L_2} = e^{-j\frac{2\pi}{L_2}}$ and $\sum_{k_1=-K_1}^{K_1} \sum_{k_2=-K_2}^{K_2}$ denotes $\sum_{k_1=-K_1}^{K_1} \sum_{k_2=-K_2}^{K_2}$.

Fig. 3 shows an example of genuine matching using the original POC function and the BLPOC function. The BLPOC function provides better discrimination capability than that of the original POC function. In the following, we describe the detailed process of the matching stage (shown in Fig. 1(a)) using the BLPOC function.

(i) Effective region extraction: Given a pair of normalized iris images $\tilde{f}(n_1, n_2)$ and $\tilde{g}(n_1, n_2)$ to be compared, the purpose of this process is to extract the effective regions $f(n_1, n_2)$ and $g(n_1, n_2)$ of the same size as illustrated in Fig. 4(a). When the extracted region becomes too small to perform image matching, we extract multiple effective sub-regions from each iris image by changing the width parameter w (Fig. 4(b)). In our experiments, we extract 6 sub-regions from an iris image by changing the parameter w as 55, 75 and 95 pixels.

(ii) Displacement alignment: This step is to align the translational displacement between the extracted regions. The displacement parameters can be obtained from the peak location of the BLPOC function $r_{fg}^{K_1 K_2}(n_1, n_2)$.

(iii) Matching score calculation: We calculate the BLPOC function between the aligned images and evaluate the matching score as the maximum correlation peak value. When multiple sub-regions are extracted as illustrated in Fig. 4(b), the matching score is calculated by taking an average for effective sub-regions. If the matching score is close to threshold value to separate genuines and impostors, we calculate the matching

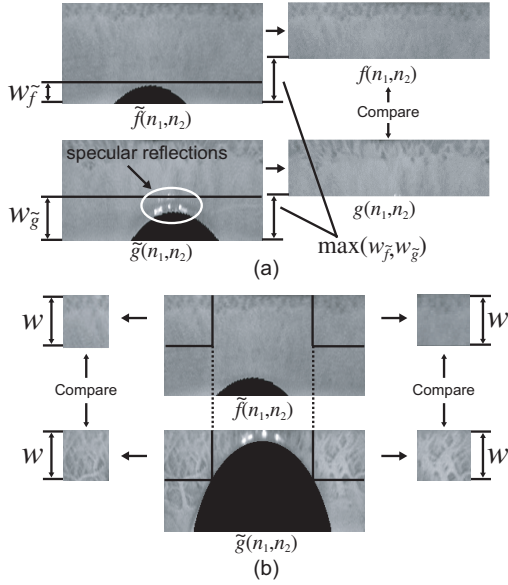


Fig. 4. Effective region extraction: (a) normal case, and (b) case when multiple sub-regions should be extracted.

score with scale correction.

C. 2D Fourier Phase Code

The proposed matching algorithm assumes the use of iris images directly in the system to achieve high recognition performance. In order to reduce the size of iris data and to prevent the visibility of individual iris images, we introduce here the idea of 2D Fourier Phase Code (FPC) for representing iris information.

2D FPC corresponds to the quantized version of phase spectrum of a normalized iris image, which is essential for phase-based iris recognition. Instead of using iris images directly, the system registers 2D FPCs as biometric data. A major problem of this approach is that 2D FPC does not contain amplitude spectrum and the actual iris image cannot be reconstructed from 2D FPC. This causes problems in “Effective Region Extraction” stage and “Displacement Alignment” stage in the flowchart shown in Fig. 1(a), since these two stages should be performed in spatial image domain.

An idea for addressing this problem is to employ pseudo iris images synthesized from the corresponding 2D FPCs in the above two stages. The pseudo iris image preserves only phase information of the original iris image. As for amplitude components, we use average amplitude spectrum computed from the given database. Formally, the pseudo iris image \tilde{f} of an iris image f is defined as the 2D IDFT of the pseudo complex spectrum \tilde{F} , whose amplitude $|\tilde{F}|$ is an average amplitude computed from many iris images and whose phase $\angle \tilde{F}$ is given by the 2D FPC of the iris image f .

Note here that we can use arbitrary chosen 2D amplitude spectra for $|\tilde{F}|$ to synthesize pseudo iris images. It is important to find an adequate amplitude spectrum, which minimizes image distortion after 2D IDFT. For example, the constant amplitude spectrum $|\tilde{F}| = 1$ is the simplest choice. However,

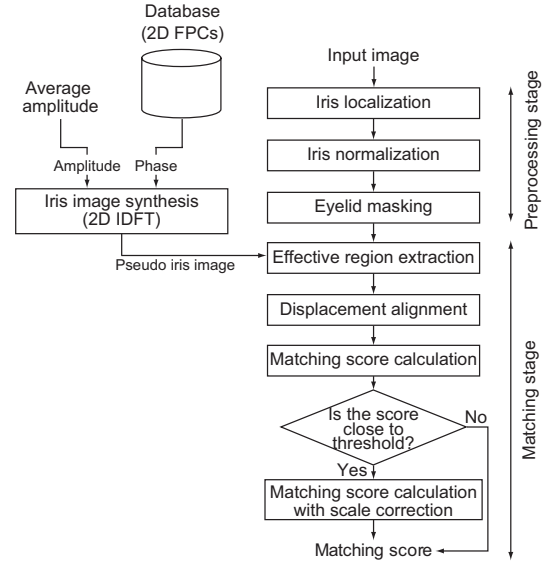


Fig. 5. Flow diagram of the proposed algorithm using 2D FPCs.

our experimental observation shows that the use of average amplitude spectrum exhibits much higher performance than the constant amplitude spectrum. Fig. 5 shows the flowchart of the iris recognition algorithm using 2D FPCs.

In general, the phase spectrum of a natural image has random values between $-\pi$ and π . Therefore, the quantization of phase components in 2D FPC (Fig. 6) does not have a significant impact on overall recognition performance. This property is particularly useful for reducing the iris data size, while keeping a sufficient level of performance. In our original algorithm, the iris region is normalized into a rectangular image block of 256×128 pixels. Assuming 8-bit (256-level) quantization of pixel value, the total data size of an iris image becomes $256 \times 128 = 32$ Kbytes. On the other hand, the size of 2D FPC with 4-bit quantization (Fig. 6(a)) can be reduced to 8 Kbytes by utilizing the symmetry of phase spectrum. Similarly, the sizes of 2D FPCs with 3-bit, 2-bit and 1-bit quantization are 6 Kbytes, 4 Kbytes and 2 Kbytes, respectively (Fig. 6(b)–(d)).

III. EXPERIMENTAL EVALUATION

This section describes a set of experiments using CASIA iris image database ver. 1.0 [7] for evaluating the performance of the proposed algorithm using 2D FPCs. This database contains 756 eye images (108 eyes and 7 images of each eye). We evaluate the genuine matching scores and the impostor matching scores for all the possible combinations (genuine: 2,268 attempts, impostor: 283,122 attempts). We compare the six different types of biometric data representation: normalized iris images (used in the original algorithm), 2D FPCs without quantization, 2D FPCs with 4-bit, 3-bit, 2-bit and 1-bit quantization. In addition, for comparison with other algorithm, we use publicly available MATLAB source code of iris recognition algorithm using 1D log-Gabor filter [8]. This software is widely used for comparison purpose recently

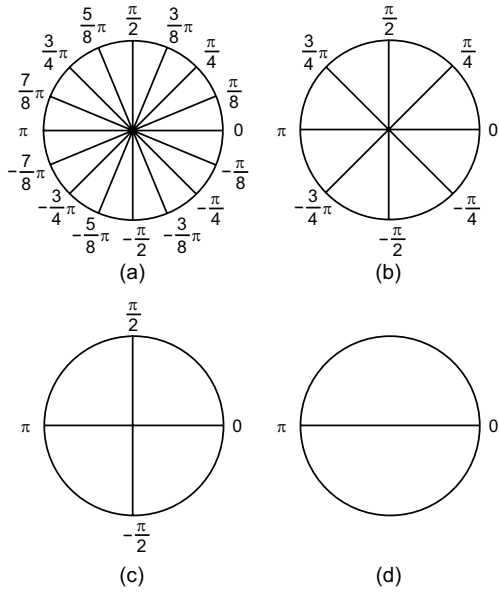


Fig. 6. Phase quantization: (a) 4-bit quantization (16 angles), (b) 3-bit quantization (8 angles), (c) 2-bit quantization (4 angles), and (d) 1-bit quantization (2 angles).

as a Daugman-like (not exactly Daugman) algorithm, which produces 1D feature vector from individual iris images. The dissimilarity between a pair of feature vectors is measured by their Hamming distance. In this source code, various parameters have already been optimized for CASIA iris image database ver. 1.0 by the author. So we modified only the preprocessing stage of the source code to our method while the matching stage remains unchanged. Thus, this test allows us to compare only the performance of matching stage. Fig. 7 shows the ROC (Receiver Operating Characteristic) curves for the algorithms. The ROC curve illustrates FNMR (False Non-Match Rate) against FMR (False Match Rate) at different thresholds on the matching score. EER (Equal Error Rate) shown in the figure is the error rate where FNMR and FMR are equal. As observed in the figure, the original algorithm achieves EER=0.0032%, while 2D FPC-based algorithms exhibit higher EER ranging from 0.16% to 2.54%. But EERs of the 2D FPC-based algorithms are still quite impressive compared with 1D log-Gabor filter approach.

These experimental results clearly demonstrate that 2D FPCs are particularly useful for implementing iris recognition devices using DSP technology. On the other hand, the original phase-based iris recognition algorithm described in [5], [6] is particularly suitable for implementing high-accuracy iris verification/identification systems, for which the recognition performance is a major concern.

IV. CONCLUSION

In this paper, we proposed an implementation-oriented approach for phase-based iris recognition. In order to reduce the size of registered iris data and to prevent the visibility of individual iris images, we introduce the idea of 2D Fourier Phase Code (FPC) for representing iris information. 2D FPC is

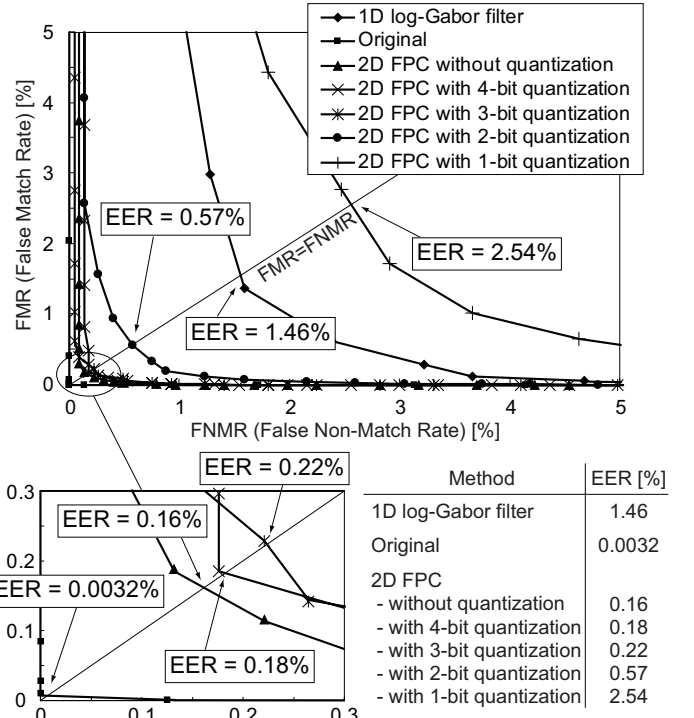


Fig. 7. ROC curves and EERs for various levels of quantization and 1D log-Gabor method.

particularly useful for implementing compact iris recognition devices using embedded microprocessors having DSP functionality. By changing the degree of phase quantization, we can optimize the trade-off between iris data size and recognition performance in a highly flexible manner.

ACKNOWLEDGMENT

Portions of the research in this paper use CASIA iris image database collected by Institute of Automation, Chinese Academy of Sciences.

REFERENCES

- [1] J. Wayman, A. Jain, D. Maltoni, and D. Maio, *Biometric Systems*, Springer, 2005.
- [2] J. Daugman, "High confidence visual recognition of persons by a test of statistical independence," *IEEE Trans. Pattern Anal. Machine Intell.*, vol. 15, no. 11, pp. 1148–1161, Nov. 1993.
- [3] R. Wildes, "Iris recognition: An emerging biometric technology," *Proc. IEEE*, vol. 85, no. 9, pp. 1348–1363, Sept. 1997.
- [4] L. Ma, T. Tan, Y. Wang, and D. Zhang, "Efficient iris recognition by characterizing key local variations," *IEEE Trans. Image Processing*, vol. 13, no. 6, pp. 739–750, June 2004.
- [5] K. Miyazawa, K. Ito, T. Aoki, K. Kobayashi, and H. Nakajima, "An efficient iris recognition algorithm using phase-based image matching," *Proc. Int. Conf. on Image Processing*, vol. II, pp. 49–52, Sept. 2005.
- [6] K. Miyazawa, K. Ito, T. Aoki, K. Kobayashi, and H. Nakajima, "A phase-based iris recognition algorithm," *Lecture Notes in Computer Science (ICB2006)*, vol. 3832, pp. 356–365, Jan. 2006.
- [7] CASIA iris image database.
<http://www.sinobiometris.com>
- [8] L. Masek and P. Kovesi, "Matlab source code for a biometric identification system based on iris patterns," *The School of Computer Science and Software Engineering, The University of Western Australia*, 2003.
<http://www.csse.uwa.edu.au/~pk/studentprojects/libor/sourcecode.html>